-RESEARCH PAPER-

International Journal of Mining and Geo-Engineering

IJMGE

IJMGE 59-3 (2025) 211-220

DOI: 10.22059/IJMGE.2025.363788.595092

Preparation of landslide risk map in Karganeh watershed, Lorestan Province, Iran

Ebrahim Karimi Sangchini [a, *], Seyed Hossein Arami [b], Ali Dastranj [c]

[a] *Soil Conservation and Watershed Management Research Department, Lorestan Agricultural and Natural Resources Research and Education Center (AREEO), Khorramabad, Iran.*

[b] *Forests and Rangelands Research Department, Khuzestan Agricultural and Natural Resources Research and Education Center, Agricultural Research Education and Extension Organization (AREEO), Ahvaz, Iran.*

[c] *Soil Conservation and Watershed Management Department, Khorasan Razavi Agricultural and Natural Resources Research and Education Center (AREEO), Mashhad. Iran.*

Article History:

Received: 23 January 2024.

Revised: 11 May 2025.

Accepted: 19 May 2025.

ABSTRACT

Mass movements are one of the natural tragedies that are more manageable than other natural disasters. Therefore, it is very important to understand this phenomenon in order to prevent the damage it can cause. Therefore, the present research was conducted in order to assess the risk of landslides and prepare a map of the severity of landslide risk in the Karganeh Watershed, Lorestan Province, Iran. Interpretation of aerial photos and field visit were used to prepare a landslide inventory map. In this research, 16 key landslide causal factors were identified to explore their spatial relationship with landslides. These factors reflect both inherent geomorphological characteristics and human influences related to landslide occurrences. Then, landslide hazard maps were built via tree models in geographic information system (GIS). Next, the information layer of the elements at risk and the degree of vulnerability of the elements were extracted. Finally, the landslide risk map was prepared by combining maps of the hazard map, elements at risk and degree of vulnerability of elements based on the general risk equation. The results presented that the (SVM) model provided greatly higher prediction accuracy of the landslide hazard map in the Karganeh Watershed via a/an (ROC) equal to 0.913. Additionally, the results of the risk map for the Karganeh Watershed indicated that 18.2% of the area is in the high-risk class. This area is equivalent to 5,349 hectares. Preparing a landslide risk map helps to focus the management work in the sectors that have a lot of risk and reduces the waste of time and money.

Keywords: *Landslide risk map, Elements at risk, Vulnerability map, Karganeh Watershed, Iran.*

1. Introduction

Numerous natural hazards and related tragedies, such as earthquakes, volcanic eruptions, tsunamis, cloudbursts, floods, and soil erosion, occur around the world. Among these, landslides are one of the most severe and frequently recurring types of natural disasters globally (Oh and Lee, 2017; Arabameri el al., 2020a; Karimi Sangchini et al., 2022). Landslide is the reason for many monetary costs and lives yearly (Kelarestaghi and Ahmadi, 2009). Every year, landslides have resulted in huge damage to life and property, including the damage of forests, fruitful cultivated land, habitation area, and network communication in addition to tourist attractions. Additionally, alteration of the Earth's surface is also responsible for devastating landslides. Consequently, landslides are accountable for huge flooding in hill areas, tsunamis in the seaside zones, and river form alterations sideways alongside geomorphic and topographical modifications (Pham el al., 2019). Consequently, landslide susceptibility mapping be able to be one of the key phases in diminishing these costs (Aleotti and Chowdhury 1999; Regmi et al. 2013; Karimi Sangchini et al. 2016). Iran has confronted numerous categories of natural threats and disasters, for example severe soil erosion through gully expansion, violent floods, and disturbing landslides. So, because of the numerous occurrences of landslides and huge financial damages, they have developed into national disasters of Iran. The landslide event in Iran has caused about 500 billion financial damage (Arabameri el al., 2020b). Essentially, the existence of the sole natural structures for example physiographic, environmental, and climatic conditions along with anthropogenic actions and their rising demand on natural resources are very susceptible to landslide action in northern part of mountainous areas in Iran (Karimi Sangchini et al., 2011; Aghda et al., 2018). Landslide susceptibility assessment is a vital procedure for the management of natural tragedies. There is no solitary method to recognize and prepare a zoning map to measure the susceptibility caused by the wide series of happenings of landslides (Chen et al., 2017a; Rahmati et al., 2018; Pourqasmi and Rahmati, 2018).

By applying logical methods, a set of accurate tools is provided for preparing and optimizing the landslide-zoning map. Additionally, these tools enhance the use of landslide forecast models, reducing issues in hazard identification and zoning (Carrara et al., 2003; Dahal et al., 2008; Bathrellos et al., 2009; Kayastha et al., 2013; Karimi Sangchini et al., 2014). In recent years, data mining models have been increasingly used because of their high accuracy and strong information processing capabilities. For example, the Artificial Neural Network is one such model (Chen et al., 2017a; Harmouzi et al., 2019; Yao et al., 2022), Logistic Regression (Hong et al., 2015; Karimi Sangchini et al., 2016;

* Corresponding author: *Tel./Fax: +989139850152; E-mail address:* E.karimi64@gmail.com (E. Karimi Sangchini).

Abedini et al., 2017; Hemasinghe et al., 2018, Shano et al., 2021; Puente-Sotomayor et al., 2021).

The random forest (RF) method is a machine learning (ML) and decision tree modelling technique. It assesses the connection between landslide occurrences and environmental factors by combining the RF results from multiple trees (Chen et al., 2017b). Among the researchers who used RF Algorithm in their studies for landslide susceptibility zoning, we can reference Zhou et al. (2021), Sevgen et al. (2019), Zhao et al. (2020), Qian et al. (2021), Sun et al. (2021) and Burak et al. (2021). The findings of these researchers' studies indicate that the RF algorithm has adequate accuracy in landslide susceptibility zoning. The maximum entropy (ME) model is another ML method that has been commonly used in recent years. Phillips et al. (2006), Convertino et al. (2013), Kim et al. (2015), Chen et al. (2017a), Kerekes et al. (2018), Pandey et al. (2020) and Barman et al. (2023) used the maximum entropy method in their studies to estimate landslide susceptibility. The results of these studies highlight the efficiency of the maximum entropy (ME) model in landslide susceptibility zoning. An additional ML method is support vector algorithm (SVM), which was used in this study for landslide susceptibility zoning. In their studies, Peng et al. (2014), Hang et al. (2015), Pham et al. (2016), Lee et al. (2017), Chen et al. (2017a), Kornejady et al. (2019), Panahi et al. (2020) and Balogun et al. (2021) conducted landslide susceptibility zoning via the support vector algorithm. The results of these researchers' studies established the usefulness of the support vector algorithm in landslide hazard zoning. Selecting the correct model that has significant accuracy and reliability can be extensively and efficiently used in the forecast and management of landslides in the text of land surveying package. In this study, an effort has been made to use the most relevant factors affecting the occurrence of landslides, in addition to new ML approaches in the study area.

Landslide risk map is calculated from the involvement of three related factors: the possibility of a landslide with a certain magnitude (landslide hazard zoning), the valued elements of risk and vulnerability. Risk elements comprise roads and water sources, buildings, agricultural actions, electricity and telephone networks (Saldivar-Sali et al., 2007; Kunlong et al., 2007; Remondo et al., 2008, Zezere et al., 2008). Damage to the contents of buildings and damage to cars on the highways can include a huge portion of the risk, but it is hard to evaluate these costs and they also lack adequate data. In addition, damage to human life (casual damage) cannot be analyzed (Enrique et al., 2008; Karimi Sangchini et al., 2015).

In this study, tree-based models of data mining algorithms were related for landslide susceptibility assessment in Karganeh Watershed. Consequently, to perform our investigation aim, 16 suitable landslides for this watershed area were used. Moreover, historic information of 95 landslide polygons was chosen to enhance development in the investigation work. Lastly, three models used in the present research have been validated via statistical examination of receiver working characteristics-area below curve (ROC-AUC). Also, in this research, the hazard, the elements at risk, the vulnerability of the elements due to the occurrence of landslides and finally the risk of landslides in the Karganeh watershed are studied simultaneously. As a result, the aim of this research is to assess the hazard with the best methods, and to assess the landslide risk via hazard map, elements at risk and the vulnerability of risk in order to manage hazard and risk in the Karganeh watershed. This could be taken as a brand-new methodology toward landslide zoning difficulties.

2. Materials and methods

2.1. Study area

The Karganeh Watershed is one of the sub-watersheds of Karkheh River, which is sited in the northeast of Khorramabad city. It is placed between 33° 25′ 12″ to 33° 37′ 12″ latitude and 48° 23′ 59″ to 48° 44′ 24″ longitude, occupying about 294.2 sq km in the Lorestan Province, west of Iran (Fig. 1). Altitude in the study area differs among 1,300 to 2,700 m. The average annual precipitation in the watershed is 469 mm. In terms of stratigraphy, Karganeh Watershed has Bakhtiari, Gachsaran, Asmari, Kashkan, Amiran, Cretaceous limestones and contemporary sediments. Around 41% of this watershed is covered by rangelands and rocky lands, forests, residual lands, agricultural lands, and orchards (nearby 59% of this watershed).

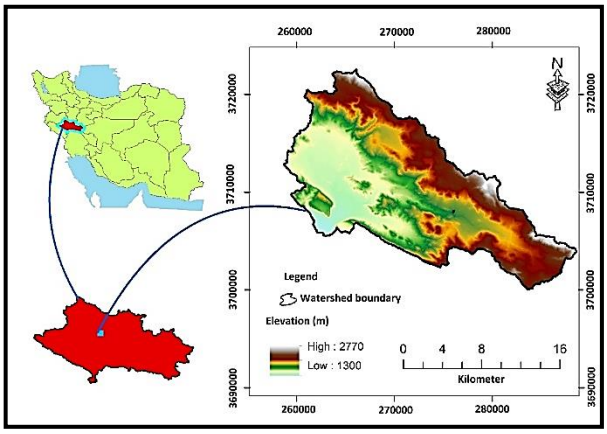

Figure 1. Geographical site of the Karganeh Watershed.

2.2. Landslide inventory map

In the present study, a landslide inventory map was prepared by field surveys, native data, and aerial photographs interpretation. To make this map for hazard assessment, one point was placed every 100 hectares. As there were numerous points with landslides, the same number of areas without landslides were taken (Figure 2).

2.3. Selection of effective factors

Elevation is an indirect factor that plays a crucial role in the occurrence of landslides. Among these factors are the amount of precipitation, temperature variations, freezing and thawing cycles, and physical and chemical weathering (Chen et al., 2017b; Kornejady et al., 2019; Karimi Sangchini, 2024). The slope aspect significantly influences factors such as moisture infiltration, slip surface angle, and soil cohesion (Devkota et al., 2013; Balogun et al., 2021). Many studies emphasize the direct role of slope and its impact on landslides (Lee et al., 2005; Kerekes et al., 2018; Panahi et al., 2020). Aspect is of particular interest in landslide studies because it plays a decisive role in the amount of rainfall and humidity, sunlight, and wind regime—all of which contribute to the initiation of displacement (Arabameri et al., 2020a; Arabameri el al., 2020b; Shano et al., 2021). Different rock units exhibit varying sensitivities to landslide occurrence; therefore, the geological factor is indispensable in all landslide-related studies and is often identified as the most critical factor in researchers' findings (Karimi Sangchini, 2014; Panahi et al., 2020). Generally, water infiltration resulting from precipitation into the slope increases pore pressure, reduces soil suction, and increases the weight of the soil mass, ultimately decreasing the soil's shear strength and predisposing the slope to failure (Harmouzi et al., 2019; Shano et al., 2021). Vegetation cover has a highly complex and contrasting role in landslide susceptibility. This role is determined by four factors, including mechanical stability provided by roots, soil moisture drainage via transpiration, additional loads from tree weight, and wind-induced failures (Sun et al., 2021). Rivers influence slope stability either through erosion or by increasing the solubility of materials due to rising water levels, which contributes to slope instability (Karimi Sangchini et al., 2016). The distance from faults or fractures and the degree of fragmentation also significantly increase the potential for slope instability (Lombardo et al., 2014; Lee et al., 2017). Human activities such as road construction and building development are among the most important factors leading to landslides in hilly areas (Kerekes et al., 2018; Arabameri et al., 2020a; Yao et al., 2022). Topographic indices quantitatively assess the influence of morphology on mass wasting processes (Kerekes et al., 2018; Pandey et al., 2020;

Arabameri et al., 2020a; Karimi Sangchini et al., 2024).

By investigating the Kerganeh watershed, 19 factors were chosen as effective factors in landslide occurrence (Mahalingam et al., 2016; Arabameri et al., 2020a; Shano et al., 2022). Tolerance and (VIF) tests were used in SPSS software version 20 to determine the most effective factors by investigating collinearity among them. Tolerance scores lower than 0.1 and VIF scores greater than 10 show collinearity between factors (Lombardo et al., 2014). The presence of collinearity between the factors reduces the accuracy of the landslide hazard map (Kohavi, 1995; Václavík and Meentemeyer, 2009; Chapi et al. 2017; Jebur et al., 2014; Mokarram et al., 2015). In the current research, VIF and (TOL) methods were applied to assess multicollinearity between the different landslide-effective factors (Lee, 2005; Devkota et al., 2013). The multicollinearity problems happen while the threshold rate of VIF is > 5 and TOL is <0.1. To compute the VIF and TOL for multicollinearity, the following equation has been used (Ozdemir, 2011).

$$TOL = 1 - R_j^2 \quad (1)$$

$$VIF = \frac{1}{TOL} \quad (2)$$

Where, R_j^2 describe coefficient of various determination of j on the forecaster variables.

The results of the collinearity test using the Tolerance and VIF indices are shown in Table 1. After the investigation, slope, slope direction, elevation classes, geology, distance from the river, distance from the road, distance from the fault, river power index (SPI) (Tien Bui et al. 2016), topographic moisture index (TWI) (Wilson et al., 2000; Grohmann et al., 2011; Hong et al., 2015; Tyagi et al., 2021) and slope length index (LS), topographic position index (TPI) (Boria et al., 2014; Kalantar et al., 2020)., topographic roughness index (TRI) and vector roughness measurement index (VRM), land use, distance from the village, and rainfall were selected as the most effective factors for landslide occurrence in the Karganeh Watershed.

2.4. Landslide hazard mapping

The maximum entropy method is one of the ML techniques and a probabilistic estimation approach that has been widely utilized in recent years across various aspects of natural resources. It is based on presence-only data (Philips et al., 2006). Originally designed for predicting species distribution, this method has gradually been adopted in other fields, such as landslide susceptibility prediction. The advantage of this method lies in its ability to predict the behavior of a species or phenomenon without requiring absence data; it utilizes a set of influencing factors (variables affecting landslide occurrence) along with presence points of the phenomenon (landslide locations for modelling) (Pandey et al., 2020). Ultimately, a model is generated with the highest capability to identify susceptible areas for landslides.

The RF model is a ML approach used for decision tree modelling (Kornejady et al., 2019). In this model, random sampling of data and variables is performed automatically and iteratively to generate a multitude of regression trees. To determine the optimal number of trees, an initial set of trees is used to produce a graph of the mean squared error (MSE) against a specific number of training and evaluation sample trees. This serves as a powerful analytical tool for exploring data and selecting the optimal number of trees in the RF model. The optimal tree count is chosen such that it minimizes the MSE while avoiding an excessive number of trees that would require extensive computational time for variable analysis. One of the primary parameters in implementing the RF model is the predictor K at each node for estimating the dependent variable (response) (Zhao et al., 2020). The model can also indicate the error associated with merging information from the generated trees via the Out-Of-Bag (OOB) error index, which can be used to optimize the number of trees for input data analysis within the software. Among the key outcomes of this model is the ranking of independent variables (factors influencing landslide occurrence) in the studied basin (Chen et al., 2019).

This model is a supervised ML technique used for classification and data separation. In other words, after defining the input data (independent variables) and target data (dependent variables), the support vector machine (SVM) algorithm analyzes the relationship between these variables (training stage) and categorizes the data into distinct groups. In the SVM algorithm, each data sample is represented as a point in an n-dimensional space on a scatter plot (where n corresponds to the number of features), with each feature value determining the coordinates of the point. A hyperplane is then drawn to segregate the different classes from each other, with the optimal separation being achieved by the hyperplane that maximizes the margin between classes (Pham et al. 2016). The core idea of this algorithm involves transforming a binary classification problem—using training points—into a higher-dimensional space to find an optimal hyperplane. Data points near this hyperplane are called support vectors. Once the decision boundary is established, it can be used to classify new data points. Equations 3 illustrates a set of training samples:

$$Xi = (i=1, 2, ..., n)\ Xi= (i = 1, 2, ..., n) \quad (3)$$

Training samples consist of two classes, Xi = ±1 Xi= ±1, indicating presence or absence, which serve as the target for the SVM model (Panahi et al., 2020; Balogun et al., 2021).

A landslide hazard map was prepared by the RF algorithm. The RF model is one of the ML methods for decision tree modelling. In this study, R software and RF package were used in order to apply the RF model in the assessment of landslide hazard (Chapi et al., 2017; Chen et al., 2019; Zhao et al., 2020). The maximum entropy model in MaxEnt software was used in order delineate landslide susceptibility zones. To apply this model, the independent variables (factors affecting the occurrence of landslides) and the dependent variables (points of occurrence of landslides) were first converted into the appropriate format and entered into the MaxEnt software environment. Based on the principle of entropy, this model forms a network of communication between independent and dependent variables (Park, 2015; Pandey et al., 2020). In this study, ModEco software and SVM algorithm were used to implement the SVM model (Pham et al., 2016). Finally, the landslide hazard map was classified into five equal-interval hazard classes, including very low, low, medium, high, and very high (Karimi Sangchini et al., 2016). The (ROC) index was used to evaluate landslide hazard models (Pontius and Schneider, 2001).

Table 1. Collinearity test between effective factors in landslides.

Factors	Tolerance	VIF	Factors	Tolerance	VIF
Slope	0.62	1.6	Topographic Position Index (TPI)	0.8	1.06
Aspect	0.58	1.8	Topographic Roughness Index (TRI)	0.73	1.53
Elevation	0.54	2.3	Vector Roughness Measure (VRM)	0.32	2.6
Geology	0.67	2.3	Soil texture	0.012	13.1
Distance from river	0.78	1.02	Distance from village	0.82	1.61
Distance from road	0.39	3.1	NDVI index	0.035	16.1
Distance from fault	0.26	3.9	Curvature Index	0.063	18.4
River Power Index (SPI)	0.44	2.7	Landuse	0.29	4.1
Topographic Wetness Index (TWI)	0.51	3.5	Precipitation	0.48	2.1
slope length (LS)	0.26	2.5			

2.1. Landslide risk map

The overall landslide risk is estimated using the equation R=H×E×V (Varnes, 1984), where R represents the risk, H is the magnitude of the hazard (susceptibility), E denotes the elements at risk (also susceptibility), and V is the vulnerability level of the elements (Zezere et al., 2008). The hazard map serves as the primary basis for assessing landslide risks in the studied basin, and ultimately, the risk map is classified accordingly (Karimi Sangchini et al., 2011). Due to the lack of temporal landslide data, the susceptibility map was used as a substitute for the risk map in the risk assessment model. When the susceptibility map is incorporated into the risk equation, the resulting risk is semi-quantitative. The elements at risk in this study include roads, buildings, fishing workshops, tourist sites, mosques, banks, health centers, power and gas transmission networks, water resources, and agricultural and pastoral activities. Damages to building contents and vehicles on roads can constitute a significant portion of the total damage; however, estimating these damages is challenging, and sufficient data are unavailable. Additionally, damages to human life (fatalities) are unquantifiable in this context. (Karimi Sangchini et al., 2011).

Vulnerability encompasses several concepts, including (1) exposure: climatic exposure indicators include increases in temperature, heavy or light rainfall, droughts, and rising sea levels. The IPCC has predicted that the impacts of global warming will manifest as potential waves of extreme heat, heavy rainfall, droughts, and a reduction in tropical regions, and rising ocean levels over time (Parry et al., 2005); (2) sensitivity: the degree of a system's sensitivity to climatic hazards depends not only on geographical conditions but also on economic and social factors such as population density and infrastructure. Sensitivity indicators may include geographical features, land use, individual characteristics, and industrial structures, including dependency on agriculture and industrial diversity; (3) Adaptive Capacity: adaptive capacity describes a system's ability to cope with the extremes of climate. Generally, adaptive capacity relates to physical resources, access to technology and information, diversity of infrastructure, institutional capabilities (both governmental and non-governmental), and resource distribution. Indicators of adaptive capacity include economic capabilities, physical infrastructure, social capital, institutional capacity, and data availability. Economic capabilities reflect the available financial resources to reduce vulnerability arising from climate change, encompassing human resources, alternative technologies, and social capital (Cutter, 1996).

To evaluate damages, smaller polygons of less than 10 hectares were merged with neighboring homogeneous polygons, forming a damage assessment map based on the landslide risk map in homogeneous polygons nearby. This map served as the basis for landslide damage evaluation in the study watershed. Residential areas (villas and rural houses), communication roads (asphalt and dirt roads), land use (forest, pasture, and agriculture), and water sources were selected as elements at risk. (Zezere et al., 2008). To calculate the vulnerability score of the elements, the existence of hazard and the conditions of each of the elements are important from the economic and ecological points of view. The elements that are in a higher hazard class have more importance and vulnerability score. To calculate the vulnerability, the combination of the intrinsic value of elements at risk and the hazard class in which these elements are located is used (Enrique et al., 2008). The final map was classified into very low, low, medium, high, and very high classes.

3. Results

3.1. Landslide inventory map

After the investigation, it was found that 95 landslides were detected in the Karganeh watershed, which had a total area of 1438 hectares (5% of the Karganeh watershed area).

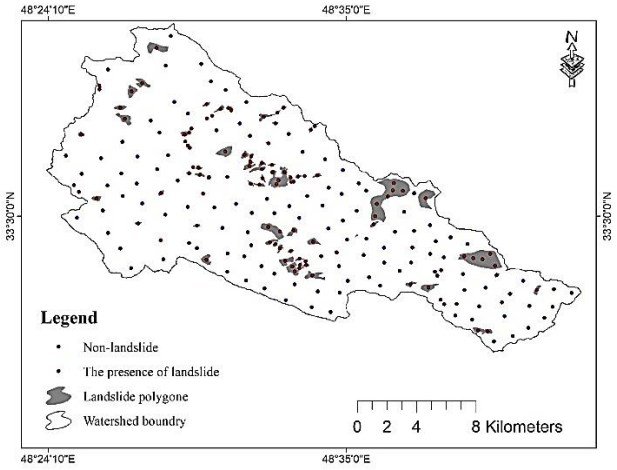

Figure 2. Landslide distribution map in the Karganeh Watershed.

3.2. Landslide hazard zonation

Using the resulting models, the landslide hazard maps were created and categorized into very low, low, medium, high, and very high classes (Table 3 and Fig. 3).

Table 2. The vulnerability core of elements at risk.

Elements at risk	Potential of elements at risk	Increase coefficient	Vulnerability number
Roads	pathway road, without infrastructure.	1	1-5
	The dirt road has infrastructure	2	1-10
	Asphalt road, with infrastructure	3	1-15
	The main road has infrastructure and increase	4	1-20
Buildings	Rural residential areas	2	1-10
	Urban residential areas	3	1-15
	Touristic, industrial areas, mosques, fishing workshop, post bank, school, mines, health center	4	1-20
Water resources	The spring	2	1-10
	Stream (rank 2 and above)	2	1-10
	Agricultural wells and pools	3	1-15
Agriculture	Rainfed agricultural	2	1-10
	The irrigated agricultural	3	1-15
	Garden	4	1-20
Natural resources	Rangelands	2	1-10
	Forests	3	1-15

Table 3. The scattering of area in diverse landslide hazard classes.

	Random Forest (RF)		Maximum Entropy (ME)		Support Vector Machine (SVM)	
Susceptibility class	Area (ha)	% Area	Area (ha)	% Area	Area (ha)	% Area
Very low	19681.29	66.9	7709.38	26.2	15240.48	51.8
Low	1691.32	5.7	7134.48	24.2	3772.63	12.8
Medium	799.74	2.7	6347.89	21.6	1774.75	6.1
High	992.39	3.4	7342.38	25	4501.64	15.3
Very high	6251.5	21.3	882.13	3	4126.74	14
Total	29416.24	100	29416.24	100	29416.24	100

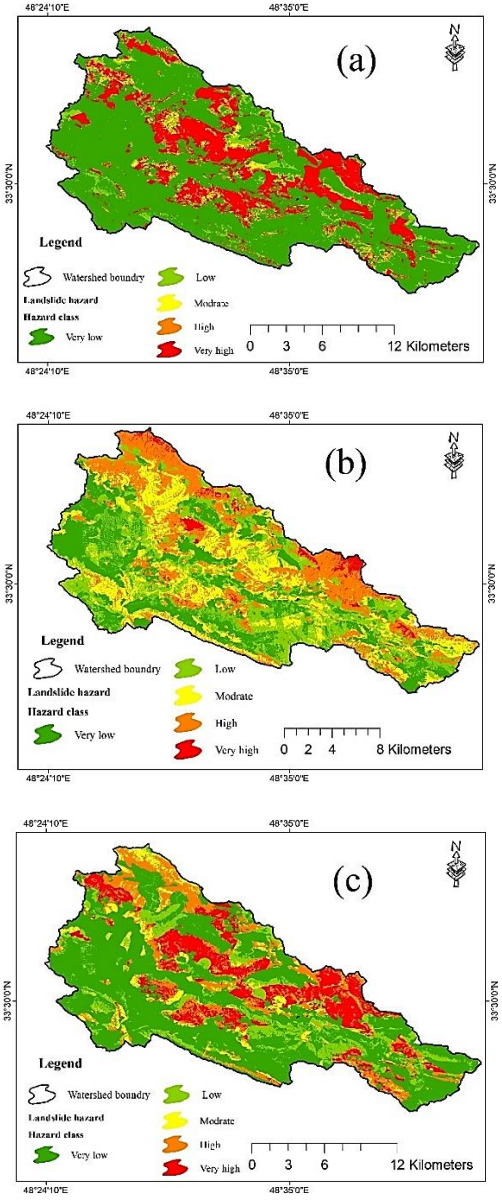

Figure 3. Landslide hazard maps based on, (a): Random Forest (RF), (b): Maximum Entropy (ME), and (c) Support Vector Machine (SVM)

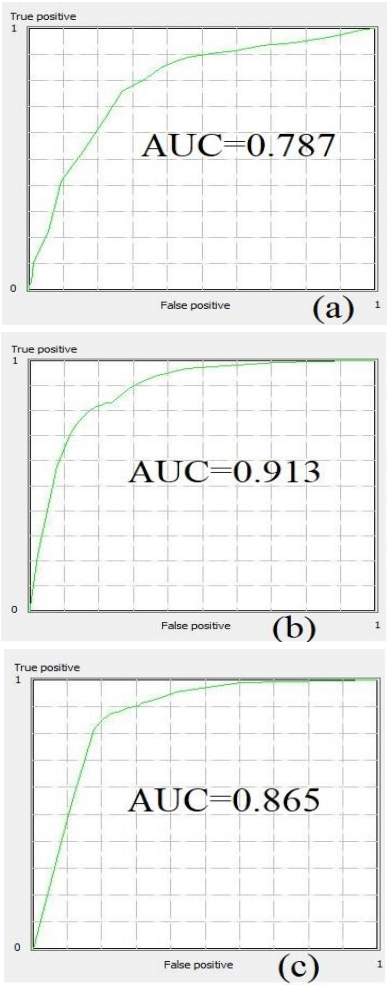

Figure 4. ROC curves (a) Maximum Entropy (ME), (b) Support Vector Machine (SVM), and (c) Random Forest (RF).

The results of the validation evaluation of the models used in this research using the ROC curve method are shown in Figure 4. The zone below the ROC index diagram for the validation of the maximum entropy model was 0.787, the area under the ROC index diagram was 0.913 for the validation of the SVM model, the area under the ROC index diagram for the validation of the RF model measurement was 0.865. This shows that the models used in zoning and determining landslide prone areas in the Karganeh Watershed have a very good capability. The SVM model with ROC equal to 0.913 was selected as the best model in landslide risk assessment in the Karganeh Watershed.

3.3. The results of landslide risk assessment

The location of pastures, forests, and agriculture were prepared from the distribution of springs, the land use map, and the number and type of residential places, the length of roads and waterways were prepared from the 1:25000 digital topographic map. Based on this information,

maps of elements at risk and vulnerability were prepared. Using the general equation, the risk number was calculated and categorized into very low, low, medium, high, and very high classes.

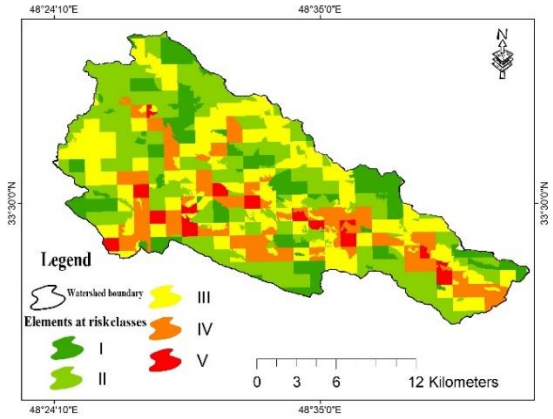

Figure 5. Element at risk map in the Karganeh Watershed.

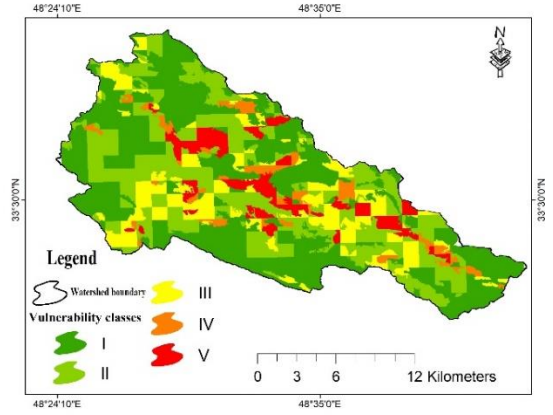

Figure 6. vulnerability map in the Karganeh Watershed.

Table 4. Elements at risk classes in the Karganeh Watershed.

Classes	Number of elements	Area (ha)	% Area
Very Low	0, 1	4663.37	15.85
Low	2	10411.55	35.39
Medium	3	8342.23	28.36
High	4	4816.22	16.37
Very High	5	1182.86	4.02
Total		29416.24	100

Table 5. Vulnerability classes in the Karganeh Watershed.

Classes	Vulnerability number	Area (ha)	% Area
Very low	0.0-18	12508.88	42.52
Low	18-36	9190.09	31.24
Medium	36-54	4192.89	14.25
High	54-72	1347.77	4.58
Very high	72-90	2176.60	7.40
Total		29416.24	100

Table 6. The delivery of zone in diverse landslide risk classes.

Class	Pixel value	Area (ha)	% Area
Very low	0-25	15049.11	51.16
Low	26-50	4617.80	15.70
Medium	51-75	4399.79	14.96
High	76-100	2407.99	8.19
Very high	101-125	2941.53	10.00
Total		29416.24	100

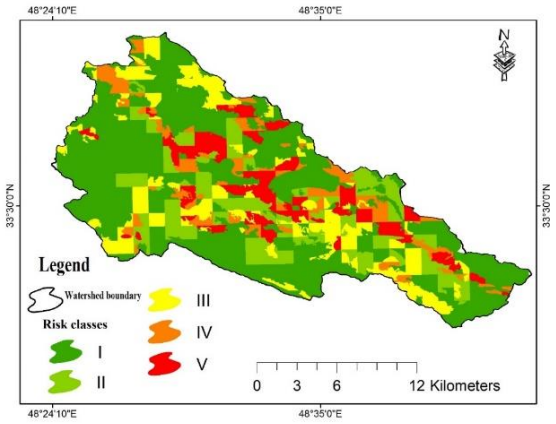

Figure 7. Risk map in the Karganeh Watershed.

4. Discussion and conclusion

In this study, it was tried to use all effective factors in order to evaluate landslide risk in Karganeh Watershed. In order to determine the best method of landslide sensitivity, three ML models, including maximum entropy, RF and SVM models were used in the Karganeh Watershed. In order to model landslide hazard, 70% of landslide points were used for model training and 30% of landslide data were used for model validation. The maximum entropy model calculates the complex distribution algorithm and by providing diverse results, it helps a lot to understand the phenomenon and process of occurrence and reaction of factors. This method is one of the quantitative methods of determining sensitivity and it is one of the models that has received a lot of attention in the last 10 years and has been used by researchers in different parts of the world. Convertino et al. (2013) in Italy and Kim et al. (2015) in South Korea have used the maximum entropy method in their studies. Based on the results obtained from this model, 50.2% of the area of the area is in the very low and low sensitivity class, 21.6% is in the medium sensitivity class, and 28% is in the high and very high sensitivity regionalization level. After evaluating this model with the ROC index, the amount of surface area under the graph in the validation stage was 0.787, this result indicates the average capability of the model in zoning and determining areas prone to landslide susceptibility in the Karganeh Watershed. The SVM model is one of the supervised ML models used to classify and separate data. The main idea of this algorithm is a binary classification using training points, which transforms the original input space into a space with higher dimensions, in order to find a desirable hyperplane. The training points that are close to the desired plane are called support vectors. Once the decision level is obtained, it can be used to estimate new data. Peng et al. (2014), Hang et al. (2015), Lee et al. (2017) and Pham et al. (2016) have used the SVM algorithm in their studies for landslide susceptibility zoning. Based on the results obtained from this model, 64.6% of the district surface area is in the very low and low sensitivity class, 6.1% is in the medium sensitivity class, and 29.3% is in the high and very high sensitivity area. The amount of surface area under the ROC index diagram was obtained at 0.913 in the validation stage, which indicates the very good capability of the model in determining areas prone to landslide susceptibility in the Karganeh Watershed. The RF model forms a cluster of decision trees. During the modelling, it involves the effective underlying factors and the evidence of landslide occurrence. Moreover, with high repetition, it removes the inefficient decision branches in the modelling process and finally continuously improves the predictions. By minimizing the prediction error, it has a very high power in predicting landslide susceptibility. Similar results have been obtained in the researches of Chen et al. (2017b), Rahmati et al. (2018), Pourqasmi, and Rahmati (2018). Based on the results obtained from this model, 72.6% of the area of the district is in the very low and low sensitivity class, 2.7% in the medium sensitivity class, and 24.7% of the area is in the high and very high

sensitivity class. The amount of surface area under the ROC index diagram was obtained at 0.865 in the validation stage, which indicates the good capability of the model in determining landslide susceptibility areas in the Karganeh Watershed. According to the results obtained from the evaluation of the models using the area under the ROC curve, the SVM model was selected as the best model in the zoning of landslide susceptibility in the Karganeh Watershed. This shows that this model has high accuracy in evaluating the landslide susceptibility in the studied area. By comparing the results obtained with the real conditions through field visits, there is a very high agreement between the results of the landslide susceptibility map using the SVM and the actual evidence in the study area. According to the landslide susceptibility map using the SVM model, the areas with high susceptibility are located on the steep slopes upstream and at high altitudes, which caused the upstream material to fall down due to the high slope and the effect of gravity. In addition, a large part of the studied area is in low slopes with agricultural and orchards, which have low and very low susceptibility in terms of landslide occurrence. After the zonation using the SVM model in the Karganeh Watershed, nearby 24.7% of the watershed area is placed in high and very high hazard classes. The results of this research also showed that the SVM model is a promising approach for landslide susceptibility modelling. The results of this research also showed that the maximum entropy model is a promising approach for landslide susceptibility modelling. This model has a map with high accuracy in identifying and separating areas sensitive to the occurrence of landslides. It helps decision makers and engineers to introduce areas with different sensitivity to landslides to build a suitable place to prevent the destruction of sediment collecting structures, management of slopes, drainage and water transfer from sensitive areas close to the implementation of the structure, development of road network and land preparation programs.

In this research, the Warren's equation (R = H.E.V) was used to evaluate landslide risk in the Karganeh Watershed. According to this equation, a hazard map (H), elements at risk map (E), and a vulnerability map (V) are needed. Hence, to prepare the risk map, the elements at risk were identified, and then, by applying the degree of vulnerability of each element, the landslide risk number was calculated from the risk equation and classified into five classes. Zezere et al. (2008) in North Lisbon in Portugal, Saldivar-Sali et al. (2007) in Baguio City, Philippines, Kunlong et al. (2007) in China, Remondo et al. (2008) in Spain used this equation to evaluate the landslide risk.

In this research, four road factors, including residential areas, water resources, agriculture, and natural resources were selected as elements at risk. Zezere et al. (2008) selected road and building as elements at risk in North Lisbon, Portugal. Enrique et al. (2008) in Quantamo, Cuba, selected houses, schools, cemeteries and roads as elements at risk. 20.4% of the Karganeh Watershed was classified as high and very high elements at risk. 12% of this watershed was placed in the class of high and very high landslide vulnerability. The reason for that is the absence of important facilities, large factories, important structures, and large recreational complex in this watershed.

Finally, according to the risk map of the study area, 18.2% of the Karganeh Watershed, equivalent to 5349.5 hectares, was located in the high and very high-risk class. 67 % of this watershed, equal to 19666.9 hectares was in the low and very low risk class. As a result, due to the presence of elements at risk in the region, most of the region has low and very low risk. In addition, this makes the management work to be concentrated on the sectors that have a lot of damage and reduces the waste of time and money.

Acknowledgements

This article is taken from a part of the results of a research project with the approved code 2-59-29-031-000489 in the Agricultural Research, Education and Extension Organization and from the respected officials of the SCWMRI and Lorestan Agricultural and Natural Resources Research and Education Center, Agricultural Research.

References

[1]. Abedini M, Ghasemyan B, Rezaei Mogaddam MH (2017) Landslide susceptibility mapping in Bijar city, Kurdistan Province, Iran: a comparative study by logistic regression and AHP models, Environmental earth sciences 76(8): 1-14.

[2]. Aghda SF; Bagheri V; Razifard M, (2018) Landslide susceptibility mapping using fuzzy logic system and its influences on mainlines in lashgarak region, Tehran, Iran, Geotechnical and Geological Engineering 36: 915–937.

[3]. Aleotti P, Chowdhury R (1999) Landslide hazard assessment: summary review and new perspectives, Bull Eng Geol Environ 58: 21–44.

[4]. Arabameri A, Karimi Sangchini E, Pal SC, Saha A, Chowdhuri I, Lee S, Tien Bui D (2020a) Novel Credal Decision Tree-Based Ensemble Approaches for Predicting the Landslide Susceptibility, Remote Sensing 12: 3389. https://doi.org/10.3390/rs12203389.

[5]. Arabameri A, Saha S, Roy J, Chen W, Blaschke T, Tien Bui D (2020b) Landslide Susceptibility Evaluation and Management Using Different Machine Learning Methods in The Gallicash River Watershed, Iran, Remote Sensing 12: 475.

[6]. Balogun AL, Rezaie F, Pham QB, Gigović L, Drobnjak S, Aina YA, Panahi M, Temitope S, Yekeen SL (2021) Spatial prediction of landslide susceptibility in western Serbia using hybrid support vector regression (SVR) with GWO, BAT and COA algorithms, Geoscience Frontiers 12 (3): 101104. https://doi.org/10.1016/j.gsf.2020.10.009.

[7]. Barman J, Ali SS, Biswas B, Das J (2023) Application of index of entropy and Geospatial techniques for landslide prediction in Lunglei district, Mizoram, India, Natural Hazards Research https://doi.org/10.1016/j.nhres.2023.06.006.

[8]. Bathrellos G.D, Kalivas DP, Skilodimou HD (2009) GIS-based landslide susceptibility mapping models applied to natural and urban planning in Trikala, Central Greece, Estudios Geológicos 65(1): 49-65. doi:10.3989/egeol.08642.036.

[9]. Boria RA, Olson LE, Goodman SM, Anderson RP (2014) Spatial filtering to reduce sampling bias can improve the performance of ecological niche models, Ecological Modelling 275: 73–77.

[10]. Burak FT, Abbaspour A, Alimohammadlou Y, Tecuci G (2021) Landslide susceptibility analyses using Random Forest, C4.5, and C5.0 with balanced and unbalanced datasets, Catena 203: 105355, https://doi.org/10.1016/j.catena.2021.105355.

[11]. Carrara A, Giovanni C, Frattini P (2003) Geomorphological and historical data in assessing landslide hazard, Earth Surface Processes and Landforms 28: 1125-1142. doi:10.1002/esp.545.

[12]. Chapi K, Singh VP, Shirzadi A, Shahabi H, Bui DT, Pham BT, Khosravi K (2017) A novel hybrid artificial intelligence approach for flood susceptibility assessment, Environmental Modelling and Software 95: 229–245.

[13]. Chen W, Pourghasemi HR, Kornejady A, Zhang N (2017a) Landslide spatial modeling: Introducing new ensembles of ANN, MaxEnt, and SVM machine learning techniques, Geoderma 305: 314-327.

[14]. Chen W, Xie X, Wang J, Pradhan B, Hong H, Bui DT, Duan Z, Ma J (2017b) A comparative study of logistic model tree, random forest and classification and regression tree models for spatial prediction of landslide susceptibility, CATENA 151: 147-160.

[15]. Chen W, Yan X, Zhao Z, Hong H, Bui DT, Pradhan B (2019)

Spatial prediction of landslide susceptibility using data mining-based kernel logistic regression, naive Bayes and RBFNetwork models for the Long County area (China), Bulletin of Engineering Geology and the Environment 78: 247–266.

[16]. Convertino M, Troccoli A, Catani F (2013) Detecting fingerprints of landslide drivers: a MaxEnt model, Journal of Geophysical Research: Earth Surface 118(3): 1367-1386.

[17]. Cutter S.L, (1996) Vulnerability to environmental hazards, Progress in Human Geography 20(4): 529-539.

[18]. Dahal R K, Hasegawa S, Nonomura S, Yamanaka M, Masuda T, Nishino K (2008) GIS-based weights-of-evidence modelling of rainfall-induced landslides in small catchments for landslide susceptibility mapping, Environmental Geology 54: 311–324.

[19]. Devkota K, Regmi A, Pourghasemi HR, Yoshida K, Pradhan B, Ryu I, Dhital M, Althuwaynee Q (2013) Landslide susceptibility mapping using certainty factor, index of entropy and logistic regression models in GIS and their comparison at Mugling–Narayanghat road section in Nepal Himalaya, Nat Hazards 65: 135-165.

[20]. Grohmann CH, Smith MJ, Riccomini C (2011) Multi-scale Analysis of Topo- graphic Surface Roughness in the Midland Valley, Scotland, IEEE Transactions on Geoscience and Remote Sensing 49:1200-1213. DOI:10.1109/TGRS.2010.2053546

[21]. Harmouzi H, Nefeslioglu HA, Rouai M, Sezer EA, Dekayir A, Gokceoglu C (2019) Landslide susceptibility mapping of the Mediterranean coastal zone of Morocco between Oued Laou and El Jebha using artificial neural networks (ANN), Arabian Journal of Geosciences 12(22):1-18.

[22]. Hemasinghe H, Rangali RS, Deshapriya NL, Samarakoon L (2018). Landslide susceptibility mapping using logistic regression model (a case study in Badulla District, Sri Lanka), Procedia engineering 212:1046-1053.

[23]. Hong H, Pradhan B, Xu C, Bui DT (2015) Spatial prediction of landslide hazard at the Yihuang area (China) using two-class kernel logistic regression, alternating decision tree and support vector machines, Catena 133: 266-281.

[24]. Jebur MN, Pradhan B, Tehrany MS (2014) Optimization of landslide conditioning factors using very high-resolution airborne laser scanning (LiDAR) data at catchment scale, Remote Sensing Environmental 152: 150–165.

[25]. Kalantar B, Ueda N, Saeidi V, Ahmadi K, Halin AA, Shabani F (2020) Landslide Susceptibility Mapping: Machine and Ensemble Learning Based on Remote Sensing Big Data, Remote Sensing 12, 1737.

[26]. Karimi Sangchini E, Arami S, Rezaii Moghadam H, Khodabakhshi Z, Jafari R (2015) Landslide Risk Assessment for Baba Heydar Watershed, Chaharmahal and Bakhtiari Province, Iran, Iranian journal of earth sciences 6(2): 121-132.

[27]. Karimi Sangchini E, Emami S, Tahmasebipour N, Pourghasemi H, Naghibi SA, Arami S, Pradhan B (2016) Assessment and comparison of combined bivariate and AHP models with logistic regression for landslide susceptibility mapping in the Chaharmahal-e-Bakhtiari Province, Iran, Arabian journal of geosciences 9 (201): 1-15.

[28]. Karimi Sangchini E, OwneghM, Sadoddin A, Mashayekhan A (2011) Probabilistic Landslide Risk Analysis and Mapping (Case Study: Chehel-Chai watershed, Golestan Province, Iran), Journal of Rangeland Science 2(1): 425-436.

Karimi Sangchini E, Salehpour Jam A, Mosaffaie J (2022) Flood risk management in Khorramabad watershed using the DPSIR framework, Natural Hazards 122 (1): 3101-3121.

[29]. Karimi Sangchini E, Arami S.H, Dastranj A. (2024). Accuracy assessment of GLM and SVM models in preparing a landslide susceptibility map (Case study: Karganeh watershed, Lorestan province), esearches in Earth Sciences 15(3: 119-136.

[30]. Kayastha P, Dhital MR, De Smedt F (2013) Evaluation and comparison of GIS based landslide susceptibility mapping procedures in Kulekhani watershed, Nepal, Journal of the Geological Society of India 81:219-231.

[31]. Kelarestaghi A, Ahmadi H (2009) Landslide susceptibility analysis with a bivariate approach and GIS in Northern Iran. Arabian journal of geosciences 2:95–101.

[32]. Kerekes A, Poszet S, Andrea GÁL (2018) Landslide susceptibility assessment using the maximum entropy model in a sector of the Cluj–Napoca Municipality, Romania, Revista de Geomorfologie 20(1):130-146.

[33]. Kim HG, Lee DK, Park C, Kil S, Son Y, Park JH (2015) Evaluating landslide hazards using RCP 4.5 and 8.5 scenarios, Environmental earth sciences 73(3):1385-1400.

[34]. Kohavi R (1995) A study of cross-validation and bootstrap for accuracy estimation and model selection, In Proceedings of the International Joint Conference on Artifcial Intelligence (IJCAI), Montreal, QC, Canada, 20–25 14:1137–1145.

[35]. Kornejady A, Pourghasemi HR, Afzali SF (2019) Presentation of RFFR new ensemble model for landslide susceptibility assessment in Iran, In Landslides: theory, practice and modelling 123-143.

[36]. Kunlong, Y. I. N., Lixia, C. H. E. N., & Zhang, G. (2007). Regional landslide hazard warning and risk assessment. Earth Science Frontiers, 14(6), 85-93.

[37]. Lee S (2005) Application of logistic regression model and its validation for landslide susceptibility mapping using GIS and remote sensing data, International Journal of Remote Sensing 26 (7): 1477–1491.

[38]. Lee S, Hong S M, Jung HS (2017) A support vector machine for landslide susceptibility mapping in Gangwon Province, Korea, Sustainability 9(1): 48.

[39]. Lombardo L, Cama M, Maerker M, Rotigliano E (2014) A test of transferability for landslides susceptibility models under extreme climatic events: Application to the Messina 2009 disaster, Natural Hazards 74:1951–1989.

[40]. Mahalingam R, Olsen MJ, O'Banion MS (2016) Evaluation of landslide susceptibility mapping techniques using lidar-derived conditioning factors (Oregon case study), Geomatics, Natural Hazards and Risk 7:1884–1907.

[41]. Mokarram M, Roshan G, Negahban S (2015) Landform classification using topography position index (Case study: Salt dome of Korsia-Darab plain, Iran), Modeling Earth Systems and Environment 1: 40.

[42]. Oh HJ, Lee S (2017) Shallow landslide susceptibility modeling using the data mining models artificial neural network and boosted tree. Applied Sciences 7: 1000.

[43]. Ozdemir A (2011) Using a binary logistic regression method and GIS for evaluating and mapping the groundwater spring potential in the Sultan Mountains (Aksehir, Turkey), Journal of Hydrology 405:123–136.

[44]. Panahi M, Gayen A, Pourghasemi HR, Rezaie F, Lee S (2020) Spatial prediction of landslide susceptibility using hybrid support vector regression (SVR) and the adaptive neuro-fuzzy

inference system (ANFIS) with various metaheuristic algorithms, Science of The Total Environment 741: 139937. https://doi.org/10.1016/j.scitotenv.2020.139937.

[45]. Pandey VK, Pourghasemi HR, Sharma MC (2020) Landslide susceptibility mapping using maximum entropy and support vector machine models along the Highway Corridor, Garhwal Himalaya, Geocarto International 35(2): 168-187.

[46]. Park N W (2015) Using maximum entropy modeling for landslide susceptibility mapping with multiple geo environmental data sets, Environmental Earth Sciences 73(3): 937-949.

[47]. Parry M, Rosenzweig C, Livermore M (2005), Climate change, global food supply and risk of hunger,Philosophical Transactions of the Royal Society of London B, Biological Sciences 360(1463): 2125-2138.

[48]. Peng L, Niu R, Huang B, Wu X, Zhao Y, Ye R (2014) Landslide susceptibility mapping based on rough set theory and support vector machines: A case of the Three Gorges area, China, Geomorphology 204:287-301.

[49]. Pham BT, Pradhan B, Bui DT, Prakash I, Dholakia MB (2016) A comparative study of different machine learning methods for landslide susceptibility assessment: A case study of Uttarakhand area (India), Environmental Modelling and Software 84:240-250.

[50]. Pham BT, Prakash I, Singh SK, Shirzadi A, Shahabi H, Tran TTT, Bui DT (2019) Landslide susceptibility modeling using Reduced Error Pruning Trees and different ensemble techniques: Hybrid machine learning approaches, Catena 175:203–218.

[51]. Phillips SJ, Anderson RP, Schapire RE (2006) Maximum entropy modeling of species geographic distributions, Ecological modelling 190(3):231-259.

[52]. Pontius RJ, Schneider LC (2001) Land-cover change model validation by an ROC method for the Ipswich watershed, Massachusetts, USA, Agriculture, Ecosystems and Environment, 85: 239–248.

[53]. Pourghasemi HR, Rahmati O (2018) Prediction of the landslide susceptibility: Which algorithm, which precision? Catena 162:177-192.

[54]. Puente-Sotomayor F, Mustafa A, Teller J (2021) Landslide Susceptibility Mapping of Urban Areas: Logistic Regression and Sensitivity Analysis applied to Quito, Ecuador, Geo environmental Disasters 8(1):1-26.

[55]. Qian H, Wang M, Liu K (2021) Rapidly assessing earthquake-induced landslide susceptibility on a global scale using random forest, Geomorphology 391:107889. https://doi.org/10.1016/j.geomorph.2021.107889.

[56]. Rahmati O, Kornejady A, Samadi M, Nobre AD, Melesse AM (2018) Development of an automated GIS tool for reproducing the HAND terrain model, Environmental modelling and software 102: 1-12.

[57]. Regmi AD, Chandra Devkota K, Yoshida K, Pradhan B, Pourghasemi HR, Kumamoto T, Akgun A (2013) Application of frequency ratio, statistical index, and weights-of-evidence models and their comparison in landslide susceptibility mapping in Central Nepal Himalaya, Arabian Journal of Geosciences 7(2):725-742.

[58]. Remondo, J., Bonachea, J., & Cendrero, A. (2008). Quantitative landslide risk assessment and mapping on the basis of recent occurrences. Geomorphology, 94(3-4), 496-507.

[59]. Saldivar-Sali, A., & Einstein, H. H. (2007). A landslide risk rating system for Baguio, Philippines. Engineering Geology, 91(2), 85-99.

[60]. Sevgen E, Kocaman S, Nefeslioglu HA, Gokceoglu C (2019) A novel performance assessment approach using photogrammetric techniques for landslide susceptibility mapping with logistic regression, ANN and random forest, Sensors 19(18): 3940.

[61]. Shano L, Raghuvanshi T K, Meten M (2021) Landslide Hazard Zonation using Logistic Regression Model: The Case of Shafe and Baso Catchments, Gamo Highland, Southern Ethiopia, Geotechnical and Geological Engineering 1-19.

[62]. Sun D, Xu J, Wen H, Wang D (2021) Assessment of landslide susceptibility mapping based on Bayesian hyperparameter optimization: A comparison between logistic regression and random forest, Engineering Geology 281: 105972.

[63]. Tien Bui D, Ho TC, Pradhan B, Pham BT, Nhu VH, Revhaug I (2016) GIS-based modeling of rainfall-induced landslides using data mining-based functional trees classifier with AdaBoost, Bagging, and MultiBoost ensemble frameworks, Environmental Earth Sciences 75: 1101.

[64]. Tyagi A, Tiwari RK, James N (2021) GIS-Based Landslide Hazard Zonation and Risk Studies Using MCDM. In Local Site Effects and Ground Failures, Springer Singapore 251-266.

[65]. Václavík T, Meentemeyer RK (2009) Invasive species distribution modeling (iSDM): Are absence data and dispersal constraints needed to predict actual distributions? Ecological Modelling 220:3248–3258.

[66]. Varnes, D. J., 1984. Landslide hazard zonation: A review of Principes and Practice, UNESCO, France, 63p.

[67]. Wilson JP, Gallant JC (2000) Terrain Analysis: Principles and Applications; John Wiley & Sons: Hoboken, NJ, USA; 524p.

[68]. Yao J, Qin S, Qiao S, Liu X, Zhang, Chen J (2022) Application of a two-step sampling strategy based on deep neural network for landslide susceptibility mapping, Bulletin of Engineering Geology and the Environment 81(4):1-20.

[69]. Zezere JL., Garcia RAC., Oliveria SC. And Reis E. (2008) Probabilistic landslide risk analysis considering direct costs in the area north of Lisbon (Portugal). Geomorphology. 94: 467–495.

[70]. Zhao L, Wu X, Niu R, Wang Y, Zhang K (2020) Using the rotation and random forest models of ensemble learning to predict landslide susceptibility, Geomatics, Natural Hazards and Risk 11(1):1542-1564.

[71]. Zhou X, Wen H, Zhang Y, Xu J, Zhang W (2021) Landslide susceptibility mapping using hybrid random forest with GeoDetector and RFE for factor optimization, Geoscience Frontiers 12(5):101211.